



HAL
open science

Mean-Field Homogenization of Time-Evolving Microstructures with Viscoelastic Phases: Application to a Simplified Micromechanical Model of Hydrating Cement Paste

Julien Sanahuja, Shun Huang

► **To cite this version:**

Julien Sanahuja, Shun Huang. Mean-Field Homogenization of Time-Evolving Microstructures with Viscoelastic Phases: Application to a Simplified Micromechanical Model of Hydrating Cement Paste. *Journal of Nanomechanics and Micromechanics*, 2017, 7 (1), pp.1-14. 10.1061/(ASCE)NM.2153-5477.0000116 . hal-03680310

HAL Id: hal-03680310

<https://hal.science/hal-03680310>

Submitted on 27 May 2022

HAL is a multi-disciplinary open access archive for the deposit and dissemination of scientific research documents, whether they are published or not. The documents may come from teaching and research institutions in France or abroad, or from public or private research centers.

L'archive ouverte pluridisciplinaire **HAL**, est destinée au dépôt et à la diffusion de documents scientifiques de niveau recherche, publiés ou non, émanant des établissements d'enseignement et de recherche français ou étrangers, des laboratoires publics ou privés.



Distributed under a Creative Commons Attribution - NonCommercial 4.0 International License

Mean-Field Homogenization of Time-Evolving Microstructures with Viscoelastic Phases: Application to a Simplified Micromechanical Model of Hydrating Cement Paste

Julien Sanahuja, Ph.D.¹; and Shun Huang²

Abstract: Homogenization of random media is a widely used practical and efficient tool to estimate the effective mechanical behavior of composite materials. However, when the microstructure evolves with respect to time, due to phase transformations, care should be taken when upscaling behaviors that themselves involve time, such as viscoelasticity. A natural assumption is to consider that the influence of microstructure evolution is negligible once the material is macroscopically loaded: it allows one to take advantage of the correspondence principle when the phases are nonaging linear viscoelastic. A new approach is proposed to overcome this limitation, building an equivalent composite replacing transforming phases by fictitious aging viscoelastic phases. This equivalent composite has a constant microstructure but is made up of aging linear viscoelastic phases. Its effective behavior can then be estimated taking advantage of recent approaches to homogenize such behaviors. Applications to cement paste are proposed, referring to a simplified morphological model. In particular, the approximation introduced when neglecting microstructure evolution is investigated. Qualitatively, compliance functions from evolving microstructure are found to be closer to the experimental ones.

Author keywords: Homogenization; Phase transformations; Evolving microstructure; Aging viscoelasticity; Cement paste; Basic creep.

Introduction

Some materials, such as concrete, exhibit a strong evolution of their microstructure along their life. During hydration of concrete, dissolution of anhydrous and precipitation of hydrates occur simultaneously, albeit more and more slowly. Evolution also occurs when concrete is exposed to ambient conditions, leading, for example, to leaching or carbonation. In all these cases, microstructure evolution is a key information to bridge the gap between physico-chemical processes occurring at smaller scales and macroscopic properties and behavior of materials. Considering microstructure evolution is thus especially critical to build less empirical behavior laws.

Homogenization techniques are widely used to upscale the mechanical behavior of composite materials with constant microstructure. When microstructure evolves, elasticity can still be up-scaled, straightforwardly working on snapshots of microstructure at given times (Bernard et al. 2003; Constantinides and Ulm 2004; Pichler et al. 2009; Sanahuja et al. 2007). However, care has to be taken for time-dependent elementary behaviors, such as nonaging linear viscoelasticity. Indeed, time appears in both morphological evolutions and behaviors of elementary phases. A common assumption is then to consider that microstructure does not evolve

any more once the macroscopic loading has been applied (Le et al. 2007; Sanahuja et al. 2009; Gu et al. 2012; Smilauer and Bažant 2010). This allows for the reuse of the well-known correspondence principle (Mandel 1966), suitable for constant microstructures made up of nonaging linear viscoelastic phases. For cementitious materials, this approach is clearly restricted to loadings at late ages, once hydration is almost stabilized and assuming the absence of other mechanisms inducing microstructure changes. To overcome this limitation, new approaches have been proposed. As far as full-field homogenization is concerned, as the microstructure is explicitly described, its evolution can be taken into account by time-stepping methods. Using as input the time-evolving microstructure of a cement paste modeled as voxels, Li et al. (2015a, b) used a dedicated finite-element code to compute the overall response to given macroscopic strain paths. Microstructure evolution was explicitly taken into account through dissolution and precipitation of voxels. As far as mean-field homogenization is concerned, Scheiner and Hellmich (2009) considered that during an infinitesimal time interval, microstructure evolves negligibly and estimated the effective creep rate of the evolving microstructure by the rate derived on the current microstructure, but subsequently kept constant, so that the correspondence principle can be used.

These approaches, numerical or semianalytical, to homogenize time-dependent microstructures whose phase behaviors are viscoelastic, are based on time-stepping algorithms and give the response to a specific loading path. A new simulation needs to be performed for each loading path investigated. This paper proposes an alternative, semianalytical approach, to estimate the effective aging viscoelastic behavior, fully characterized by the compliance or relaxation tensors as functions of two time variables. This has recently been made possible thanks to a micromechanical extension (Sanahuja 2014; Sanahuja and Di Ciaccio 2015) of Bažant solidification theory (Bažant 1977, 1979; Bažant and Prasanna 1989; Carol

¹Edf lab, Site des Renardieres, Route de Sens, Ecuelles, 77250 Moret sur Loing, France (corresponding author). E-mail: julien.sanahuja@edf.fr

²Edf lab, Site des Renardieres, Route de Sens, Ecuelles, 77250 Moret sur Loing, France. E-mail: shun-s.huang@edf.fr

and Bažant 1993) and to mean-field homogenization of aging linear viscoelastic behaviors (Sanahuja 2013; Lavergne et al. 2016). These developments have recently been applied to cementitious materials (Honorio et al. 2016).

The approach proposed in this paper is general and could be applied to any composite material undergoing phase transformations (dissolution, precipitation, or conversion from solid to solid) that induce microstructure evolution. This microstructure evolution is assumed to be independent of the local stresses or strains. In other words, this evolution is known in advance. The application proposed in this paper is restricted to aging basic creep of a cement paste due to hydration, as aging basic creep is an important feature of concrete behavior (Briffaut et al. 2012).

The paper is organized as follows. First, a time-evolving morphological model of hydrating cement paste is proposed. Anhydrous, hydrates, and capillary pores are considered, and a description of their spatial distribution as a function of time is proposed. This model is clearly a simplification of the genuine complexity of cement paste microstructure, but it allows for the illustration of developments presented in the next sections without unnecessary technical complications. Then, phases are considered as elastic, which allows for performing classic homogenization on snapshots of microstructure. Basics of mean-field homogenization in elasticity are recalled for the sake of completeness, and the effective Young's modulus of cement paste is estimated as a function of both the water-to-cement ratio and the hydration degree. Analyzing these results, limitations of the chosen simplified morphological model are pointed out, especially regarding prediction of setting. The last two sections are devoted to nonaging linear viscoelastic phases. First, the microstructure is considered as frozen (i.e., it does not evolve any more) once the macroscopic loading step has been applied. This allows for taking advantage of the correspondence principle, and the approach is recalled for the sake of completeness. However, applicability to cement pastes is restricted to late age loadings as in this case, hydration can be considered as nearly stabilized. The last section constitutes the main originality of the paper. The complete evolution of microstructure is considered, combining micromechanical extensions of Bažant solidification theory and aging linear viscoelastic mean-field homogenization. Eventually, several prospects are proposed to improve application of this new aging approach to cement pastes.

Simplified Evolving Morphological Model for Hydrating Cement Paste

The microstructure of cement pastes is made up of more than 10 phases (Lothenbach and Winnefeld 2006) categorized as either anhydrous, hydrates, or additives. Moreover, the morphology of hydrated phases, and especially of the main one for portland cements, calcium silicate hydrates (C-S-H), is highly complex [see Richardson (2000), Diamond (2004), Juenger et al. (2003), and Lothenbach et al. (2011), to name a few references]. This morphology is difficult to both observe and model. Addressing the question of microstructure of cement pastes and its evolution, is out of scope of this paper. Thus, a simplified point of view is adopted here: both anhydrous and hydrates are not detailed but considered as single phases. In other words, only three phases coexist: anhydrous (subscript a), hydrates (subscript h), and capillary porosity (subscript p). As the drained behavior is sought, capillary water is disregarded.

The aim of this paper is to propose a mean-field homogenization method to take into account microstructure evolution. The three-phases composition is simple enough to present the approach without unnecessary technical complications.

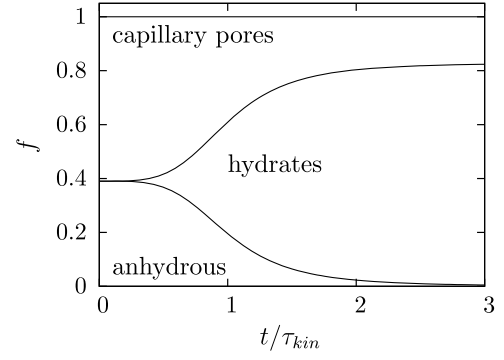


Fig. 1. Evolution of cumulative volume fractions of anhydrous, hydrates, and pores ($n_{kin} = 4$, $w/c = 0.5$)

Volume Fractions Evolution: Hydration Model

During hydration, as a function of time, anhydrous progressively dissolve and hydrates precipitate. The well-known Powers model (Powers and Brownyard 1946) is adopted to estimate the volume fractions as functions of the hydration degree α (defined as the amount of anhydrous that has reacted over the amount of initial anhydrous)

$$\begin{aligned} f_a(\alpha) &= \frac{0.32(1-\alpha)}{w/c + 0.32}, & f_h(\alpha) &= \frac{0.68\alpha}{w/c + 0.32}, & \text{and} \\ f_p(\alpha) &= \frac{w/c - 0.36\alpha}{w/c + 0.32} \end{aligned} \quad (1)$$

where w/c = water-to-cement mass ratio. An empirical kinetic model is adopted to relate the hydration degree to time

$$\alpha(t) = \frac{(t/\tau_{kin})^{n_{kin}}}{1 + (t/\tau_{kin})^{n_{kin}}} \alpha_{max}, \quad \text{where } \alpha_{max} = \min\left(\frac{w/c}{0.42}, 1\right) \quad (2)$$

where τ_{kin} and n_{kin} = kinetics characteristic time and exponent. The theoretical maximum reachable hydration degree α_{max} is also estimated from the Powers model.

The volume fractions evolution is plotted in Fig. 1, for $w/c = 0.5$ and $n_{kin} = 4$. As expected, the amount of anhydrous decreases with time, and the capillary porosity also decreases, as hydration is a space-filling process (the volume of hydrates produced is higher than the volume of anhydrous consumed).

A crude approximation of hydration and kinetics is adopted here for the sake of simplicity. More advanced models can be used, as drop-in replacements, as soon as they provide volume fractions of phases as a function of time.

Morphological Model and Its Evolution during Hydration

The volume fractions evolution being modeled, the next question to address regards the spatial distribution of the phases, that is the morphology of the composite material. The cement paste is described at any given time as a polycrystal-like assemblage. Each cell of the latter is thus occupied by either anhydrous, hydrates, or capillary porosity. Although simplified, this morphological model is rather commonly encountered (Bernard et al. 2003; Stefan et al. 2010).

The evolution of this morphology now needs to be described. The volume of hydrates produced during an increment of time being higher than the volume of consumed anhydrous, the former is split in two subvolumes:

- One part directly replaces the dissolved anhydrous; and
- The other part precipitates into capillary porosity.

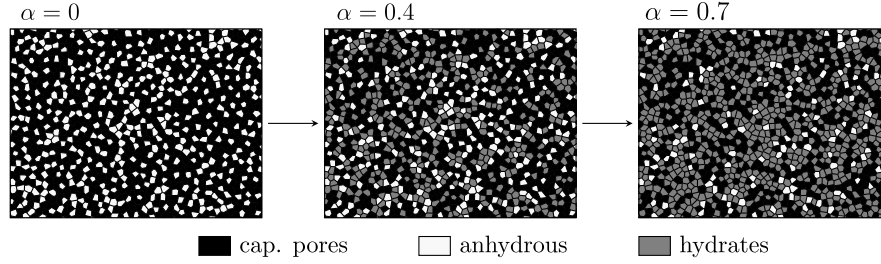


Fig. 2. Schematic two-dimensional representation of the evolving microstructure considered to model cement paste ($w/c = 0.6$)

the first part is assumed to occupy the same volume as left by dissolved anhydrous, and the second part complements the first one, up to the total amount of hydrates produced. At the scale of cement paste, these phase transformations are assumed to affect random cells. At the scale of the individual cell, these transformations are assumed to occur instantly, so that each cell is homogeneous at any given time. A schematic representation of this evolving morphological model is depicted in Fig. 2.

Effective Elastic Stiffness of Evolving Microstructure

In this section, the phases' behavior is restricted to linear elasticity. As the elastic behavior does not involve time, it is straightforward to estimate, at any given time, the effective stiffness of the composite material, from a snapshot of its morphology. The latter being constant, usual homogenization procedures can be used. The basic principle is briefly recalled here; for more details see, for example, Zaoui (2002) and Dormieux et al. (2006).

Introduction to Mean-Field Homogenization in Elasticity

The general case of a n phases composite is considered in this subsection. Phase i occupies the domain $\Omega_i(t)$, which depends on time t due to the evolving nature of the morphology. The volume fraction and stiffness tensor of phase i are respectively denoted by $f_i(t)$ and \mathbb{C}_i .

At any given time u (different notation from t , to emphasize that u is a given parameter), the set of equations to solve on the representative elementary volume (REV) Ω , with kinetic uniform boundary conditions (macroscopic strain \mathbf{E}), is

$$\boldsymbol{\varepsilon}(\underline{x}) = \mathbf{grad}^s[\underline{\xi}(\underline{x})], \quad \underline{x} \in \Omega \quad (3)$$

$$\mathbf{div}[\boldsymbol{\sigma}(\underline{x})] = \mathbf{0}, \quad \underline{x} \in \Omega$$

$$\boldsymbol{\sigma}(\underline{x}) = \mathbb{C}(\underline{x}, u) : \boldsymbol{\varepsilon}(\underline{x}), \quad \underline{x} \in \Omega$$

$$\underline{\xi}(\underline{x}) = \mathbf{E} \cdot \underline{x}, \quad \underline{x} \in \partial\Omega$$

where $\mathbf{grad}^s(\cdot)$ = symmetric part of gradient, and the local stiffness is defined by

$$\mathbb{C}(\underline{x}, t) = \sum_{i=1}^n \mathbb{C}_i \chi_i(\underline{x}, t) \quad (4)$$

where $\chi_i(\underline{x}, t)$ = characteristic function of phase i : $\chi_i(\underline{x}, t) = 1$ when $\underline{x} \in \Omega_i(t)$, and 0 otherwise.

Considering a snapshot of the evolving microstructure, that is at a fixed u , the homogenization problem Eq. (3) is the same as a

classic one with constant microstructure. The linear nature of the homogenization problem Eq. (3) with respect to the loading parameter \mathbf{E} allows one to define the so-called strain localization tensor \mathbb{A}_u , relating the microscopic to the macroscopic strain

$$\boldsymbol{\varepsilon}(\underline{x}) = \mathbb{A}_u(\underline{x}) : \mathbf{E} \quad (5)$$

the subscript indicates that \mathbb{A}_u depends on u through the current morphology at this time. The effective stiffness then derives from the application of the local behavior and from spatially averaging the microscopic stress to get the macroscopic stress

$$\mathbb{C}^{\text{eff}}(u) = \langle \mathbb{C}(\underline{x}, u) : \mathbb{A}_u(\underline{x}) \rangle = \sum_{i=1}^n f_i(u) \mathbb{C}_i : \langle \mathbb{A}_u(\underline{x}) \rangle_{\Omega_i(u)} \quad (6)$$

where $\langle \cdot \rangle$ respectively $\langle \cdot \rangle_{\Omega_i(u)}$ denoting the spatial average over Ω respectively $\Omega_i(u)$. The effective stiffness \mathbb{C}^{eff} depends on u through volume fractions f_i , phase domains Ω_i , and the localization tensor field \mathbb{A}_u .

Self-Consistent Scheme for Cement Paste

The morphology being assumed as polycrystalline at any given time, the self-consistent scheme (Budiansky 1965; Hill 1965) is the most adequate one to estimate the effective stiffness of cement paste, from the current volume fractions of anhydrous, hydrates, and pores. The behavior of these phases is assumed to be isotropic, with bulk and shear moduli k_i , g_i for phase $i \in \{a, h, p\}$. The derivation of the self-consistent scheme, with three families of spherical particles, is recalled here for the sake of completeness. The dependencies on the current time u are omitted to lighten notations.

The average strain in each phase i is estimated as the strain arising in a sphere made up of the same phase, embedded in an infinite medium characterized by the sought effective stiffness \mathbb{C}_{SC} , with kinematic uniform (\mathbf{E}_0) boundary conditions (Fig. 3). This is an Eshelby inhomogeneity problem (Eshelby 1957), whose solution is

$$\langle \boldsymbol{\varepsilon} \rangle_i = \mathbb{A}_i^{SC} : \mathbf{E}_0 \quad \text{with} \quad \mathbb{A}_i^{SC} = [\mathbb{I} + \mathbb{P}_{SC}^{\text{sph}} : (\mathbb{C}_i - \mathbb{C}_{SC})]^{-1} \quad (7)$$

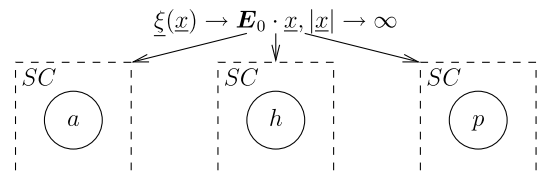


Fig. 3. Auxiliary problems to solve to implement the self-consistent scheme; anhydrous, hydrates, and pore space being represented by spherical shapes

where \mathbb{A}_i^{SC} = strain localization tensor on a sphere of stiffness \mathbb{C}_i embedded into an infinite medium of stiffness \mathbb{C}_{SC} . It involves the Hill tensor \mathbb{P}_{SC}^{sph} of a sphere in a medium of stiffness \mathbb{C}_{SC} . As both the elementary phases and the morphology are isotropic, the effective stiffness is expected to be isotropic. Consequently, the Hill tensor is also isotropic. It is also the case for the strain localization tensor, which can be written as $\mathbb{A}_i^{SC} = A_{iJ}^{SC} \mathbb{J} + A_{iK}^{SC} \mathbb{K}$, with

$$A_{iJ}^{SC} = \left(1 + \frac{3k_{SC}}{3k_{SC} + 4g_{SC}} \frac{k_i - k_{SC}}{k_{SC}} \right)^{-1} \quad (8)$$

$$A_{iK}^{SC} = \left(1 + \frac{6}{5} \frac{k_{SC} + 2g_{SC}}{3k_{SC} + 4g_{SC}} \frac{g_i - g_{SC}}{g_{SC}} \right)^{-1}$$

where k_{SC} and g_{SC} = effective bulk and shear moduli.

The average strain in the whole REV is the weighted average of the average strains in each phase

$$\mathbf{E} = \langle \boldsymbol{\varepsilon} \rangle = \sum_{i \in \{a,h,p\}} f_i \langle \boldsymbol{\varepsilon} \rangle_{\Omega_i} \quad (9)$$

the average stress in the whole REV can be written in a similar way, and eliminating the reference strain \mathbf{E}_0 from the average stress and strain yields the implicit expression of the effective stiffness as estimated from the self-consistent scheme

$$\mathbb{C}_{SC} = \left(\sum_{i \in \{a,h,p\}} f_i \mathbb{C}_i : \mathbb{A}_i^{SC} \right) : \left(\sum_{i \in \{a,h,p\}} f_i \mathbb{A}_i^{SC} \right)^{-1} \quad (10)$$

the latter is a nonlinear equation on the effective stiffness \mathbb{C}_{SC} , as the strain localization tensor \mathbb{A}_i^{SC} itself depends on the latter through Eq. (8). This tensorial equation only involves isotropic tensors. It can thus be projected on \mathbb{J} and \mathbb{K} to yield a system of two nonlinear equations on the effective bulk and shear moduli

$$k_{SC} = \frac{\sum_{i \in \{a,h,p\}} f_i k_i A_{iJ}^{SC}}{\sum_{i \in \{a,h,p\}} f_i A_{iJ}^{SC}} \quad \text{and} \quad g_{SC} = \frac{\sum_{i \in \{a,h,p\}} f_i g_i A_{iK}^{SC}}{\sum_{i \in \{a,h,p\}} f_i A_{iK}^{SC}} \quad (11)$$

Evolution of Elasticity of Cement Paste

Two kinds of input data are required in Eq. (11): the current values of the volume fractions f_i and the bulk and shear moduli k_i, g_i . Volume fractions are provided by the Powers model in Eq. (1). The elementary phases' elastic properties come from nano-indentation measurements (Velez et al. 2001; Velez and Sorrentino 2001) and are gathered in Table 1. The effective Young's modulus of hydrating cement paste is plotted as a function of the degree of hydration for various w/c ratios in Fig. 4(a).

As expected, the effective Young's modulus of paste increases with the hydration degree, and is higher for lower w/c ratios. Moreover, the micromechanical model is able to describe the setting mechanism: below a critical degree of hydration α^c , the effective stiffness is 0, and for $\alpha \geq \alpha^c$, it increases from 0. This feature comes from a well-known property of the underlying self-consistent scheme: to get a solid effective behavior, the total solid volume fraction $f_a + f_h$ has to reach 1/2. This condition can be translated to the expression of the critical degree of hydration as a function of the w/c ratio, referring to the Powers model in Eq. (1)

$$\alpha^c = \frac{w/c - 0.32}{0.72} \quad (12)$$

Discussion on the Critical Degree of Hydration

The setting degree of hydration can be difficult to directly measure experimentally, due to difficulties to perform classical mechanical tests on cementitious materials at very early ages. Torrenti and Benboudjema (2005) proposed an approach to estimate it, from compressive strength measurements for various hydration degrees, reported by Taplin (1959) and Byfors (1980). Namely, the strength dependence with respect to the hydration degree is approximated by an affine function, whose intersection with the 0-strength axis provides an estimate of the setting hydration degree. However, this estimate can be considered as an upper bound, as a few data points indicate nonzero strength (a couple of MPa) for hydration degrees lower than this estimate. Thus, at early age, strength does not increase with respect to the hydration degree according to an affine law, but rather in a smoother way, according to a concave upward curve. Indeed, Pichler et al. (2009) reported experimental

Table 1. Material and Kinetics Parameters Used in Applications

Phase	E (GPa)	ν	τ/τ_{kin}	ν^v	n_{kin}
Anhydrous	[135, (Velez et al. 2001)]	[0.3, (Velez et al. 2001)]	N/A	N/A	—
Hydrates	[31, (Velez and Sorrentino 2001)]	[0.24, (Velez and Sorrentino 2001)]	3	0.2	4
Capillary pores	0	N/A	N/A	N/A	—

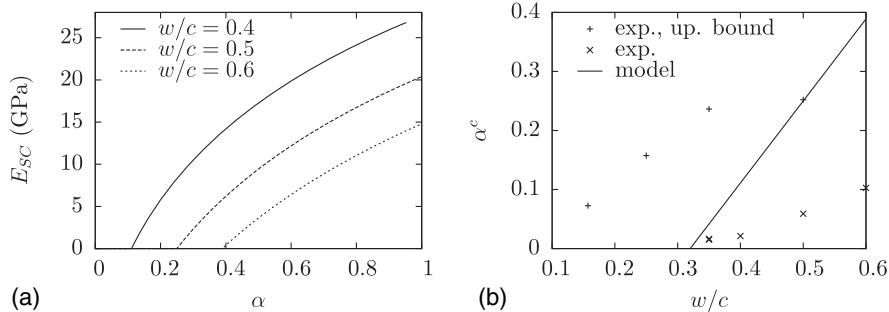


Fig. 4. (a) Effective Young's modulus of cement paste, estimated as a function of hydration degree for various w/c ratios; (b) critical degree of hydration, at setting, estimated from this model and experimentally

setting degrees of hydration from Boumiz et al. (1996) and Sun et al. (2005), which are much lower than those from Torrenti and Benboudjema (2005).

This is further confirmed by more recent experimental works. Still regarding compressive strength, Pichler et al. (2013) measured a few MPa for a $w/c = 0.42$ paste at $\alpha \approx 0.1$. Classical mechanical tests can only, by nature, be performed on already set samples. To overcome this limitation, Azenha et al. (2010) developed the elasticity modulus measurement based on ambient response method (EMM-ARM) technique, which allows one to continuously monitor the Young's modulus of cementitious materials, from the fluid state. This technique has been used to estimate the setting time of cement pastes (Maia et al. 2012a), and combined with estimates of the degree of hydration through chemical shrinkage measurements (Maia et al. 2012b), to relate the Young's modulus to the hydration degree. Nonzero stiffness ($E \approx 0.2$ GPa) has been measured for hydration degrees as low as $\alpha \approx 0.05$ on pastes prepared with w/c ratios ranging between 0.4 and 0.5.

These experimental results allow for assessing the critical hydration degree estimated by the morphological model adopted here, and to highlight its limitations [Fig. 4(b): experimental results from Torrenti and Benboudjema (2005) and Pichler et al. (2009) are reported using respectively, + and × dots]:

- Instantaneous setting (at $\alpha = 0$, before even starting hydration) occurs for $w/c < 0.32$; in this case the initial volume fraction of anhydrous is higher than 1/2. This limitation has already been pointed out by Bernard et al. (2003);
- At $w/c > 0.35$, the setting degree of hydration is overestimated, and at $w/c = 0.5$ it happens to correspond to the upper bound proposed by Torrenti and Benboudjema (2005); and
- The predicted stiffness evolution does not follow a concave upward curve just after setting.

these limitations mainly come from the simplified nature of the adopted morphological model.

Discussion on the Morphological Model

The aim of this paper is to propose a mean-field homogenization approach to estimate the effective aging viscoelastic behavior of time-evolving microstructures. To focus on the presentation of the approach rather than on technical complications, the morphological model has been deliberately chosen as a simplistic representation of cement pastes. Future works include improvements of this microstructure description. A few possibilities are recalled here, based on cement paste morphological models that have proven realistic enough to provide relevant estimates of other effective mechanical properties, such as stiffness, strength, and (nonaging) creep.

From the proposed model, which considers spherical particles and every phase at the same scale, several improvements are possible:

- Considering nonspherical shapes for hydrate particles, such as needles (Stora et al. 2006; Pichler et al. 2009; Pichler and Hellmich 2011; Pichler et al. 2013; Termkhajornkit et al. 2014) or platelets (Stora et al. 2006; Sanahuja et al. 2007). As shown on stiffness predictions (Pichler et al. 2009), considering C-S-H solid particles as needles (prolates of infinite aspect ratio) allowed to predict $\alpha_c = 0$ for $w/c > 0.32$, thus underestimating the critical hydration degree rather than overestimating it (case of spherical particles). Still, for $w/c < 0.32$, these models predict a positive Young's modulus even before starting hydration ($\alpha = 0$).
- Considering a multiscale microstructure, that is introducing a scale separation between C-S-H particles and clinker grains

(and possibly other hydrate particles such as portlandite) (Constantinides and Ulm 2004; Stora et al. 2006; Sanahuja et al. 2007; Pichler and Hellmich 2011; Gu et al. 2012; Pichler et al. 2013; Termkhajornkit et al. 2014). Combined with aspherical C-S-H solid particles, this allowed one to overcome the instantaneous setting [$E(\alpha = 0) > 0$], irrespective of the w/c ratio (Pichler and Hellmich 2011; Sanahuja et al. 2007) and to get a Young's modulus evolution starting with upward concavity (Pichler and Hellmich 2011). Furthermore, considering hydrate particles as oblates (Sanahuja et al. 2007) or prolates (Sanahuja et al. 2008) of finite aspect ratio allowed to predict a nonzero critical hydration degree, whose dependence on w/c is parametrized by the particles aspect ratio. Still, the onset of Young's modulus evolution is rather affine, but this can be improved considering a multiscale pore space in the hydrates matrix (Sanahuja et al. 2007).

- Considering two types of C-S-H, namely high-density and low-density, either homogenized to provide a matrix embedding cement grains (Constantinides and Ulm 2004) or respectively considered as inner (surrounding cement grains) and outer products (acting as a matrix embedding cement grains surrounded by inner products) (Sanahuja et al. 2007).

Going back to the scope of this paper, as the adopted model is not able to predict a concave upward onset of Young's modulus, its α_c predictions are still compared to the experimental estimates of Torrenti and Benboudjema (2005) [see + dots in Fig. 4(b)]. At $w/c \approx 0.5$, both approaches happen to be consistent: viscoelastic simulations will focus on this specific water-to-cement ratio.

Effective Viscoelastic Behavior of Evolving Microstructure: "Frozen Microstructure" Approximation

The phases behavior is now considered as nonaging linear viscoelastic. Contrary to the elastic case, this behavior now involves time. Upscaling is no longer as straightforward as considering a snapshot of the microstructure at a given time and performing homogenization on this snapshot. As the domains occupied by phases evolve with respect to time, a specific procedure will be proposed in the next section.

For now, a usual simplification [see Le et al. (2007), Sanahuja et al. (2009), and Gu et al. (2012) for mean-field homogenization or Smilauer and Bažant (2010) for full-field homogenization] is taken advantage of: to estimate the effective response of the evolving composite, the microstructure is considered as frozen once the strain step has been applied. As microstructure becomes constant, classical homogenization of nonaging linear viscoelastic behaviors can be taken advantage of. The latter is briefly recalled in the next subsection.

Introduction to Nonaging Linear Viscoelasticity Homogenization of Constant Microstructures

In this subsection, the REV is considered to be made up of n nonaging linear viscoelastic phases, without any evolution of its microstructure. The set of equations to solve on the REV, with kinetic uniform boundary conditions [macroscopic strain $\mathbf{E}(t)$, now depending on time], is

$$\boldsymbol{\varepsilon}(\underline{x}, t) = \mathbf{grad}^s[\underline{\xi}(\underline{x}, t)], \quad \underline{x} \in \Omega \quad (13)$$

$$\mathbf{div}[\boldsymbol{\sigma}(\underline{x}, t)] = \underline{0}, \quad \underline{x} \in \Omega$$

$$\boldsymbol{\sigma}(\underline{x}, t) = \int_{t'=-\infty}^t \mathbb{C}(\underline{x}, t-t') : d\boldsymbol{\varepsilon}(\underline{x}, t'), \quad \underline{x} \in \Omega$$

$$\underline{\xi}(\underline{x}, t) = \mathbf{E}(t) \cdot \underline{x}, \quad \underline{x} \in \partial\Omega$$

where the local relaxation tensor is defined by

$$\mathbb{C}(\underline{x}, t-t') = \sum_{i=1}^n \mathbb{C}_i(t-t') \chi_i(\underline{x}) \quad (14)$$

where $\chi_i(\underline{x})$ = characteristic function of phase i .

The classic approach to solve this problem is to take advantage of the correspondence principle (Mandel 1966): The Laplace-Carson transform changes nonaging linear viscoelastic behaviors into elastic ones. The Laplace-Carson transform of function $f(t)$ is $f^*(p) = p\mathcal{L}_f(p)$ with the Laplace transform $\mathcal{L}_f(p) = \int_{-\infty}^{\infty} f(t)e^{-pt} dt$.

Applying the Laplace-Carson transform to the set of Eq. (13) yields, taking advantage of the main properties of this transform (linearity and transformation of convolutions into products)

$$\boldsymbol{\varepsilon}^*(\underline{x}, p) = \mathbf{grad}^s[\underline{\xi}^*(\underline{x}, p)], \quad \underline{x} \in \Omega \quad (15)$$

$$\mathbf{div}[\boldsymbol{\sigma}^*(\underline{x}, p)] = \underline{0}, \quad \underline{x} \in \Omega$$

$$\boldsymbol{\sigma}^*(\underline{x}, p) = \mathbb{C}^*(\underline{x}, p) : \boldsymbol{\varepsilon}^*(\underline{x}, p), \quad \underline{x} \in \Omega$$

$$\underline{\xi}^*(\underline{x}, p) = \mathbf{E}^*(p) \cdot \underline{x}, \quad \underline{x} \in \partial\Omega$$

and where the Laplace-Carson transform of the local relaxation tensor is

$$\mathbb{C}^*(\underline{x}, p) = \sum_{i=1}^n \mathbb{C}_i^*(p) \chi_i(\underline{x}) \quad (16)$$

for each value of the Laplace variable p , in the Laplace-Carson domain, this problem is equivalent to the elastic one in Eq. (3).

Consequently, estimates from elastic homogenization schemes can be directly reused, formally replacing stiffness tensors by the Laplace-Carson transforms of the relaxation tensors. This yields the effective relaxation tensor in the Laplace-Carson domain $\mathbb{C}^{\text{eff}*}(p)$. The effective nonaging relaxation tensor in the time domain $\mathbb{C}^{\text{eff}}(t)$ is then obtained by inversion of the Laplace transform. The latter can be performed analytically only in the simplest cases (in terms of both morphology and phase behaviors). In the general case, inversion can be performed numerically, for example using the Stehfest algorithm (Abate and Whitt 2006; Gaver 1966; Stehfest 1970)

$$f(t) \approx \frac{\ln 2}{t} \sum_{k=1}^{2M} \zeta_k \mathcal{L}_f\left(k \frac{\ln 2}{t}\right) \quad (17)$$

with the weights

$$\zeta_k = \frac{(-1)^{M+k}}{M!} \sum_{j=\text{floor}((k+1)/2)}^{\min(k,M)} j^{M+1} \binom{M}{j} \binom{2j}{j} \binom{j}{k-j} \quad (18)$$

where $\text{floor}(x)$ = floor function, giving the highest integer lower or equal to x ; and $\binom{n}{k}$ = binomial coefficient. Further computations are performed with $M = 10$, which has been found to be a good compromise with respect to the accuracy required for evaluation in the Laplace domain of the function to be inverted.

“Frozen Microstructure” Homogenization

The evolving microstructure with nonaging linear viscoelastic phases is now considered. The “frozen microstructure” simplification consists in assuming that microstructure does not evolve any more after a given time u . The average stress response to a macroscopic strain starting at time u is sought. The macroscopic strain \mathbf{E} is thus equal to $\mathbf{0}$ for $t < u$. The microscopic strain and stress fields are then also equal to $\mathbf{0}$ for $t < u$. The frozen microstructure assumption can be expressed as: for $t \geq u$, $\Omega_i(t) = \Omega_i(u)$. Consequently, the relaxation tensor field across the REV can be written as

$$\mathbb{C}(\underline{x}, t-t') = \sum_{i=1}^n \mathbb{C}_i(t-t') \chi_i(\underline{x}, u) \quad \text{for } t \geq t' \geq u \quad (19)$$

u being fixed, this local relaxation tensor has the same expression as Eq. (14). As $\boldsymbol{\varepsilon}(t) = \boldsymbol{\sigma}(t) = \mathbf{0}$ for $t < u$, the fact that the microstructure still evolves for $t < u$ does not matter. In other words, Eqs. (13) and (14) still apply here, quantities starting to be non-0 from time u instead of from time 0.

The homogenization process, using the correspondence principle, as recalled previously, can then be taken advantage of to estimate the nonaging effective stiffness tensor $\mathbb{C}_u^{\text{eff}, \text{frozen}}(t-u)$. The latter has been indexed by u to emphasize the fact that it depends on the given time u through the phases' distribution at time u . Repeating this process for various values of u yields approximations of the effective relaxation and compliance tensors, as

$$\mathbb{C}^{\text{eff}}(t, u) \approx \mathbb{C}_u^{\text{eff}, \text{frozen}}(t-u) \quad \text{and} \quad \mathbb{S}^{\text{eff}}(t, u) \approx \mathbb{S}_u^{\text{eff}, \text{frozen}}(t-u) \quad (20)$$

where $\mathbb{S}_u^{\text{eff}, \text{frozen}}$ = inverse of $\mathbb{C}_u^{\text{eff}, \text{frozen}}$ in the sense of nonaging linear viscoelasticity. This inversion can be straightforwardly performed in the Laplace-Carson domain. Note that one nonaging linear viscoelastic homogenization computation is required per value of u .

Application to the Self-Consistent Scheme for Cement Paste

At a given time u , the morphology of the cement paste is characterized by the volume fractions $f_i(u)$. As previously recalled, the equations on the effective bulk and shear moduli established in elasticity in Eq. (11) can be reused here, replacing elastic moduli by Laplace-Carson transforms of the nonaging linear viscoelastic relaxation functions

$$k_{SC}^*(p) = \frac{\sum_{i \in \{a,h,p\}} f_i(u) k_i^*(p) A_{ij}^{SC*}(p)}{\sum_{i \in \{a,h,p\}} f_i(u) A_{ij}^{SC*}(p)} \quad (21)$$

$$g_{SC}^*(p) = \frac{\sum_{i \in \{a,h,p\}} f_i(u) g_i^*(p) A_{ik}^{SC*}(p)}{\sum_{i \in \{a,h,p\}} f_i(u) A_{ik}^{SC*}(p)}$$

note that as u = fixed parameter; and $f_i(u)$ = constant that is not affected by the Laplace-Carson transform. The components of the strain localization tensor are obtained similarly from Eq. (8)

$$A_{ij}^{SC*}(p) = \left[1 + \frac{3k_{SC}^*(p)}{3k_{SC}^*(p) + 4g_{SC}^*(p)} \frac{k_i^*(p) - k_{SC}^*(p)}{k_{SC}^*(p)} \right]^{-1} \quad (22)$$

$$A_{ik}^{SC*}(p) = \left[1 + \frac{6k_{SC}^*(p) + 2g_{SC}^*(p)}{5k_{SC}^*(p) + 4g_{SC}^*(p)} \frac{g_i^*(p) - g_{SC}^*(p)}{g_{SC}^*(p)} \right]^{-1}$$

resolution of Eq. (21) and Laplace-Carson inversion yield the nonaging effective bulk $k_u^{SC, \text{frozen}}(t-u)$ and shear $g_u^{SC, \text{frozen}}(t-u)$ relaxation functions of the frozen microstructure when $t > u$. Repeating the process for various times u allows for deriving approximations of the aging bulk and shear relaxation and compliance functions, as in Eq. (20).

“Frozen Microstructure” Approximation of Effective Creep of Cement Paste

The elementary behavior of anhydrous is elastic. For the sake of simplicity, both bulk and shear behaviors of hydrates are represented by the Maxwell model (hydrates’ viscoelastic behavior is discussed in the next subsection)

$$C_h(t) = 3k_h(t)\mathbb{J} + 2g_h(t)\mathbb{K} \quad (23)$$

with the bulk and shear relaxation functions

$$k_h(t) = k_h e^{-k_h t / \eta_h} H(t) \quad \text{and} \quad g_h(t) = g_h e^{-g_h t / \gamma_h} H(t) \quad (24)$$

where H = Heaviside function. The constants k_h , g_h , respectively, η_h , γ_h are the bulk and shear stiffness respectively, viscosities. This behavior can be alternatively defined from the elastic Young’s modulus E_h and Poisson ratio ν_h and from the viscous characteristic time τ_h and Poisson ratio ν_h^v

$$\begin{aligned} k_h &= \frac{E_h}{3(1-2\nu_h)}, & g_h &= \frac{E_h}{2(1+\nu_h)}, \\ \eta_h &= \frac{\tau_h E_h}{3(1-2\nu_h^v)}, & \gamma_h &= \frac{\tau_h E_h}{2(1+\nu_h^v)} \end{aligned} \quad (25)$$

the Laplace-Carson transform of Eq. (24) yields the bulk and shear relaxations in the Laplace-Carson domain

$$k_h^*(p) = \frac{1}{1/k_h + 1/(\eta_h p)} \quad \text{and} \quad g_h^*(p) = \frac{1}{1/g_h + 1/(\gamma_h p)} \quad (26)$$

numerical values of material parameters are gathered in Table 1; the viscous characteristics of hydrates are arbitrarily chosen for this preliminary application. Times are scaled by the kinetics characteristic time τ_{kin} .

The effective uniaxial compliance functions, obtained for various loading times u , are plotted in Fig. 5 as plain lines. The evolution of the initial elastic strain, obtained as the inverse of the

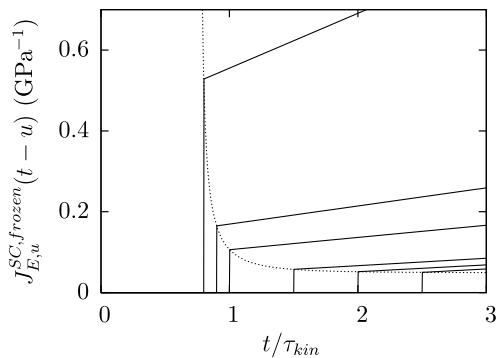


Fig. 5. Plain lines: effective uniaxial compliance functions of cement paste, approximated from frozen microstructure, plotted for various stress loading times u ($w/c = 0.5$); dotted line: initial elastic strain estimated from elasticity homogenization

effective Young’s modulus (see section dedicated to elasticity), is also plotted as a dotted line. The latter is consistent with the effective uniaxial compliance functions.

Taking into account the particular microstructure at the loading time u allows for the derivation of an aging effective behavior. However, the latter is approximate as microstructure is assumed to be frozen for $t \geq u$. To evaluate the amount of approximation induced by this assumption, microstructure evolution is completely taken into account in the last section.

Discussion on Hydrates Elementary Viscoelastic Behavior

For the sake of simplicity, hydrates’ elementary viscoelastic behavior has been represented by a Maxwell model. However, any non-aging linear viscoelastic behavior can be used, provided that the relaxation moduli are known in the Laplace-Carson domain. Regarding the relevant behavior to use, it can be derived following a bottom-up approach, taking advantage of micromechanics, starting from the creep mechanism at the microscale or nano-scale. Consensus on the latter seems not to be reached yet, and many hypotheses can be found in the literature (Bažant 2001), among which are transfers between capillary and adsorbed water (Wittmann 1982), water transfers to newly created microcracks (Rossi et al. 2012), and viscous sliding between C-S-H sheets (Tamtsia and Beaudoin 2000). Discussing the relevance of these micromechanisms is way beyond the scope of this paper.

Still, if the viscous sliding mechanism is chosen, recent works would allow for estimating the appropriate nonaging linear viscoelastic behavior to use at the hydrates’ scale (instead of the simplified Maxwell model considered in this paper):

- Considering that C-S-H solid particles are made up of a stack of elementary sheets sliding one onto the other, with a Maxwell behavior, the effective bulk and shear creep functions of a porous gel made up of such particles can be estimated from a self-consistent scheme (Sanahuja and Dormieux 2010). The asymptotic behavior (finite strain or asymptotic strain rate) is found to be dependent on both porosity and aspect ratio of solid particles.
- Considering viscous sliding surfaces embedded into an elastic matrix, Shahidi et al. (2014) derived the effective viscoelastic behavior of such a material. Equivalent stiffness and viscosities of simple rheological models have also been derived as functions of the matrix stiffness and interfaces viscosity, size, and density (Shahidi et al. 2016). Then, Eq. (26) can be replaced by the latter.

Alternatively, the hydrates’ viscoelastic behavior can be identified following a top-down approach, taking advantage of experimental data at the cement paste scale. Indeed, classical basic creep tests on cement pastes provide the compliance of cement paste when loaded at a given age, see, for example, Tamtsia and Beaudoin (2000), Tamtsia et al. (2004), and Le Roy (1995). The appropriate hydrate behavior can then be back-analyzed using a micromechanical model [see Sanahuja et al. (2009) where the sliding characteristic time of C-S-H sheets has been fit on cement paste creep measurements from Le Roy (1995)]. However, these classical tests only provide the compliance function at a given loading age. More precisely, one sample and one test are required for each loading age, prohibiting extensive characterization of aging creep. Recently, Irfan-ul-Hassan et al. (2016) proposed a new technique to characterize the aging viscoelastic behavior of cement pastes from short creep tests repeated on the same sample. Parameters of a power-law creep function are calibrated on experimental results and are given as a function of either time or hydration

degree. These results could be back-analyzed to estimate the elementary behavior of hydrates.

Effective Viscoelastic Behavior of Evolving Microstructure: Taking into Account the Complete Evolution

The aim of this section is to propose an approach that does not rely on a frozen microstructure, that is, to consider the complete evolution of microstructure as the composite material is loaded. For the sake of simplicity, the approach is not illustrated on a generic n phases composite, but directly on cement paste.

Homogenization of Evolving Microstructure with Viscoelastic Phases

As microstructure evolves with respect to time, classic homogenization of random media (such as the correspondence principle with the Laplace-Carson transform) cannot be straightforwardly used in the framework of viscoelasticity. Still, the solidification theory from Bažant (1977, 1979), Bažant and Prasanna (1989), and Carol and Bažant (1993) represents a promising source of inspiration, as it allows for deriving the effective aging linear viscoelastic behavior arising from the progressive precipitation of parallel layers of nonaging viscoelastic material. To be applied to cement paste, this theory needs to be extended in two directions:

- To consider more general precipitation mechanisms than the parallel arrangement of layers; and
- To also consider the solid (anhydrous) to solid (hydrates) phase transformation.

in this subsection, no particular morphology of the cement paste is assumed.

Instead of considering a snapshot of the evolving morphology at a given time t , the phase transformations occurring at a point \underline{x} of the cement paste REV are investigated. As described in the first section, dedicated to morphology, depending on the position of this point, one of these transformations can occur:

- Material at this point stays anhydrous;
- Transformation from anhydrous to hydrates (solid-to-solid transformation);
- Transformation from pore space to hydrates (precipitation); and
- Material at this point stays as pore space.

the subdomains affected by these transformations are respectively denoted by $\Omega_{a \rightarrow a}$, $\Omega_{a \rightarrow h}$, $\Omega_{p \rightarrow h}$, and $\Omega_{p \rightarrow p}$; they constitute a partition of the REV Ω . The idea of the proposed extension of Bažant solidification theory is to affect an equivalent aging linear viscoelastic behavior to each point in the REV. In the subdomain $\Omega_{a \rightarrow h}$, the field $t_{a \rightarrow h}(\underline{x})$ is introduced to represent the time at which transformation from anhydrous to hydrates occurs at point \underline{x} . This field is supposed to be known as it can be derived from

the description of the evolving morphology. The field $t_{p \rightarrow h}(\underline{x})$ is similarly defined as the precipitation time at \underline{x} in $\Omega_{p \rightarrow h}$.

In $\Omega_{p \rightarrow h}$, precipitation occurs. As in Bažant solidification theory, hydrates are assumed to precipitate in a zero-stress state. The equivalent mechanical behavior at point \underline{x} is identified through the stress response to strain steps starting at various times [Fig. 6(a)].

If the strain step occurs before precipitation time $t_{p \rightarrow h}(\underline{x})$, the point \underline{x} behaves as pore space: stress stays at $\mathbf{0}$ even after precipitation, as hydrates are assumed to precipitate in a stress-free state. If the strain step occurs after precipitation time, the nonaging viscoelastic behavior of hydrates is obviously retrieved. Thus, the equivalent aging behavior is a tensorial generalization of the one that can be used for one layer of Bažant's solidifying composite

$$\mathbb{C}_{p \rightarrow h}(\underline{x}, t, t') = \mathbb{C}_h(t - t')H[t' - t_{p \rightarrow h}(\underline{x})] \quad (27)$$

here, the hydrate behavior is nonaging linear viscoelastic [relaxation $\mathbb{C}_h(t - t')$], but note that no technical reason limits the approach to nonaging behaviors.

In $\Omega_{a \rightarrow h}$, a solid (anhydrous)-to-solid (hydrates) transformation occurs. This dissolution-precipitation process has not been considered by the original Bažant solidification theory. As adopted by Li et al. (2015b) for full-field simulations of cement paste creep, a quasi-instant phase transform process is assumed, involving dissolution shortly followed by precipitation. That is, anhydrous are first dissolved, then, after a short time, hydrates precipitate to occupy the domain left by anhydrous. This short time separating dissolution and precipitation is assumed to be negligible with respect to other characteristic times of the model (related to global hydration kinetics and to the hydrates viscoelastic behavior). As the volume of hydrates replacing anhydrous is here assumed to be equal to the volume of dissolved anhydrous (the complement volume precipitating in pore space), hydrates are considered to precipitate in a zero-stress state. This is clearly a simplifying assumption; in reality, hydrates precipitating in place of anhydrous may be subjected to stress, as crystals growing in pores (Scherer 1999) and due to confinement effects related to the expansive nature of the transformation from anhydrous to hydrates (Scherer 2004). Also, the current stress state may affect both dissolution (Correns 1949) and precipitation (Avramov 2007) processes and their kinetics. These effects (growing hydrates subjected to stress and influence of the stress state on dissolution and precipitation processes) are neglected in this simplified first approach and constitute sources of improvement for future works.

If the strain step occurs before dissolution-precipitation time $t_{a \rightarrow h}(\underline{x})$, the stress is first equal to the elastic stress (stiffness \mathbb{C}_a) in the anhydrous phase, then drops to $\mathbf{0}$ at transformation time, as anhydrous are dissolved and, shortly after, replaced by hydrates that precipitate in a zero-stress state [Fig. 6(b)]. If the strain step occurs after dissolution-precipitation time, the nonaging

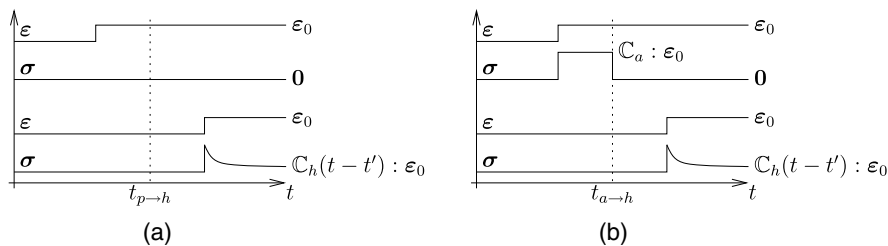


Fig. 6. Definition of equivalent aging linear viscoelastic behavior to represent (a) precipitation and (b) dissolution-precipitation phase transformation processes occurring at a given time, through stress responses to strain steps starting before or after transformation time

viscoelastic behavior of hydrates is obviously retrieved. The fictitious aging relaxation tensor is thus completely defined from these relaxation tests

$$\begin{aligned} \mathbb{C}_{a \rightarrow h}(\underline{x}, t, t') &= \mathbb{C}_a H(t - t') H[t_{a \rightarrow h}(\underline{x}) - t] H[t_{a \rightarrow h}(\underline{x}) - t'] \\ &\quad + \mathbb{C}_h(t - t') H[t' - t_{a \rightarrow h}(\underline{x})] \end{aligned} \quad (28)$$

Thus, an equivalent composite is built, affecting to each point \underline{x} a fictitious aging viscoelastic behavior equivalent to the behavior at the same point \underline{x} in the real composite undergoing microstructure evolution

$$\mathbb{C}(\underline{x}, t, t') = \begin{cases} \mathbb{C}_a H(t - t'), & \underline{x} \in \Omega_{a \rightarrow a} \\ \mathbb{C}_{a \rightarrow h}(\underline{x}, t, t'), & \underline{x} \in \Omega_{a \rightarrow h} \\ \mathbb{C}_{p \rightarrow h}(\underline{x}, t, t'), & \underline{x} \in \Omega_{p \rightarrow h} \\ 0, & \underline{x} \in \Omega_{p \rightarrow p} \end{cases} \quad (29)$$

the equivalent composite has a constant microstructure, and its microscopic behavior is aging linear viscoelastic. The constant nature of microstructure now allows for taking advantage of mean-field homogenization. Still, in $\Omega_{a \rightarrow h}$ and $\Omega_{p \rightarrow h}$, the relaxation tensor continuously depends on position \underline{x} , through the transformation time. As this prevents homogenization, it is necessary to replace this continuum by a finite number of phases. The idea is to gather points into equal-volume subdomains, according to their transformation times.

The proposed approach is illustrated on $\Omega_{p \rightarrow h}$. Fig. 7 shows the volume fraction evolution of hydrates precipitating into pore space, as a plain line. The dashed line shows the discretized volume fraction of hydrates precipitating considered with $N = 3$ subdomains. The subdomain $\Omega_{p \rightarrow h}^i$, $i = 1, \dots, N$ contains the points precipitating during the time interval corresponding to $f_{p \rightarrow h}^{\max}(i-1)/N \leq f_{p \rightarrow h}(t) < f_{p \rightarrow h}^{\max}i/N$, where $f_{p \rightarrow h}^{\max}$ is the maximum, final value of $f_{p \rightarrow h}(t)$ over the time interval of the entire simulation. The discretization consists in considering that this whole subdomain precipitates at time $t_{p \rightarrow h}^i$ such that $f_{p \rightarrow h}(t_{p \rightarrow h}^i) = f_{p \rightarrow h}^{\max}(i-1/2)/N$. The same process is repeated to subdivide the domain $\Omega_{a \rightarrow h}$ into N subdomains $\Omega_{a \rightarrow h}^i$.

Thus, the equivalent composite is subdivided into $2N + 2$ phases:

- One phase for $\Omega_{a \rightarrow a}$;
- N phases for $\Omega_{a \rightarrow h}^i$, $i = 1 \dots N$;
- N phases for $\Omega_{p \rightarrow h}^i$, $i = 1 \dots N$; and
- One phase for $\Omega_{p \rightarrow p}$.

the phases associated to $\Omega_{a \rightarrow a}$ and $\Omega_{p \rightarrow p}$ are also qualified as fictitious so that the $2N + 2$ phases of the equivalent composite can be

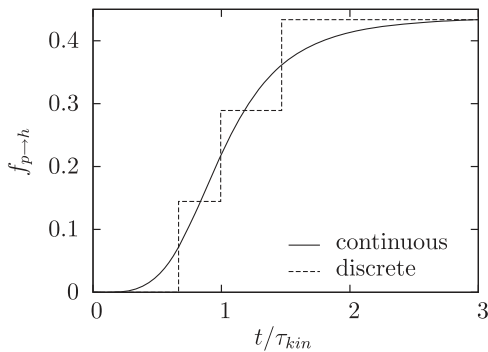


Fig. 7. Volume fraction of hydrates precipitating into pores: continuous and discretized for $N = 3$ ($w/c = 0.5$)

collectively described as fictitious phases. The effective behavior of this multiphase equivalent composite is expected, when $N \rightarrow \infty$, to converge towards the effective behavior of the continuous equivalent composite. The latter has the same local behavior, at any point \underline{x} , as the evolving composite.

The multiphase equivalent composite, having a constant microstructure, can now be homogenized, taking advantage of recent approaches to upscale aging linear viscoelastic behaviors.

Introduction to Homogenization of Aging Linear Viscoelastic Composites

Among the recent approaches (Ricaud and Masson 2009; Masson et al. 2012; Sanahuja 2013) to homogenize aging linear viscoelastic composites, Sanahuja (2013) is flexible enough to directly use as inputs the fictitious behaviors introduced to represent phase transformations [relaxation tensors in Eqs. (27) and (28)].

The morphology of the equivalent composite suggests resorting to a self-consistent scheme to homogenize its $2N + 2$ fictitious phases, using spherical shapes. Only the main expressions, useful for implementation, are reproduced here; for more details see Sanahuja (2013).

The homogenization problem to solve is the same as Eq. (13), except that the microscopic behavior is now aging linear viscoelastic

$$\boldsymbol{\sigma}(\underline{x}, t) = \int_{t'=-\infty}^t \mathbb{C}(\underline{x}, t, t') : d\boldsymbol{\epsilon}(\underline{x}, t') \quad (30)$$

where the relaxation tensor field is homogeneous per fictitious phase

$$\mathbb{C}(\underline{x}, t, t') = \sum_{i=1}^{2N+2} \mathbb{C}_i(t, t') \chi_i(\underline{x}) \quad (31)$$

where $\chi_i(\underline{x})$ = characteristic function of fictitious phase i in the equivalent composite. As shown in Sanahuja (2013), elastic homogenization can be extended to aging linear viscoelasticity when the inclusions are spherical. The equations to solve to get the self-consistent estimates of the effective bulk and shear relaxations have the same structure as Eq. (11)

$$k^{SC} = \left(\sum_{i=1}^{2N+2} f_i k_i \circ A_{iJ}^{SC} \right) \circ \left(\sum_{i=1}^{2N+2} f_i A_{iJ}^{SC} \right)^{-1} \quad (32)$$

$$g^{SC} = \left(\sum_{i=1}^{2N+2} f_i g_i \circ A_{iK}^{SC} \right) \circ \left(\sum_{i=1}^{2N+2} f_i A_{iK}^{SC} \right)^{-1}$$

where $\circ =$ Volterra integral product $f(t, \cdot) \circ x(\cdot) = \int_{t'=-\infty}^t f(t, t') dx(t')$ (Volterra 1887, 1959), “ -1 ” its inverse, i iterates over the fictitious phases, k_i and g_i depend on times t, t' and are the bulk and shear relaxations functions of fictitious phase i , and f_i is the constant (as the equivalent composite has a constant morphology) volume fraction of phase i . The components A_{iJ}^{SC} and A_{iK}^{SC} of the strain localization tensor are also functions of t, t' and have to be carefully derived solving the Eshelby inhomogeneity problem with aging linear viscoelastic phases, resorting to a displacement approach (Sanahuja 2013)

$$A_{iJ}^{SC} = (3k_i + 4g_{SC})^{-1} \circ (3k_{SC} + 4g_{SC}) \quad (33)$$

$$\begin{aligned} A_{iK}^{SC} &= H + 2(2H + 3D_{SC}) \circ [2g_i \circ (2H + 3D_{SC}) \\ &\quad + g_{SC} \circ (6H - D_{SC})]^{-1} \circ (g_{SC} - g_i) \end{aligned} \quad (34)$$

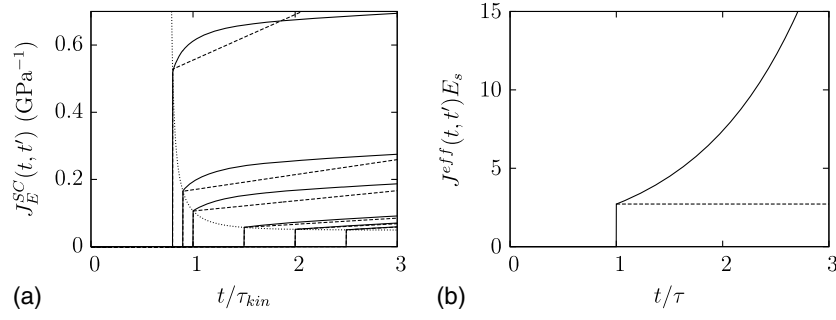


Fig. 8. (a) Effective uniaxial compliance functions of cement paste ($w/c = 0.5$), plotted for various stress loading times t' : considering full evolution of microstructure with $N = 100$ fictitious phases (plain lines), and assuming a frozen microstructure (dashed lines); dotted line represents the initial elastic strain; (b) effective compliance function of dissolving parallel elastic layers, when $f_s(t) = e^{-t/\tau}$, plotted for stress loading time $t'/\tau = 1$ considering full evolution of microstructure (plain line) or a frozen microstructure (dashed line)

with

$$D_{SC} = (k_{SC} + g_{SC})^{-1} \circ \frac{2}{3} g_{SC} \quad (35)$$

these expressions involve the Volterra integral product \circ and its inverse. To evaluate them in practice, the integral is approximated using the trapezoidal rule following Bažant (1972), so that relaxation functions are converted to matrices, whose components are defined as

$$2f_{i,j} = \begin{cases} f(t_0, 0) + f(t_0, t_0), & i = j = 0 \\ f(t_i, 0) - f(t_i, t_1), & i \geq 1, j = 0 \\ f(t_i, t_{j-1}) - f(t_i, t_{j+1}), & i \geq 2, 1 \leq j \leq i-1 \\ f(t_i, t_{i-1}) + f(t_i, t_i), & i \geq 1, j = i \\ 0, & 1 \leq i+1 \leq j \leq n \end{cases} \quad (36)$$

the Volterra product becomes a straightforward product between square matrices, and its inverse becomes matrix inversion. Solving the matrix equations obtained from Eq. (32) yields the matrix representation [as defined by Eq. (36)] of the effective bulk and shear relaxation functions. The latter define the complete effective behavior. The response to any loading path can then be postprocessed from these matrices and the time discretization of this loading path (Sanahuja 2013).

Application to Aging Creep of Cement Paste due to Hydration

The effective aging uniaxial compliance function is plotted in Fig. 8(a) as plain lines. Compliance functions obtained from the frozen microstructure approximation are also reported as dashed lines. The initial elastic strain is plotted as a dotted line. Before the critical degree of hydration is reached at t^c , the effective Young's modulus is 0, so there is no point plotting the compliance function for loading times $t' < t^c$.

Both approaches (frozen and evolving microstructure) are consistent with the initial elastic strain as estimated from elastic homogenization. Both compliance functions are very close when loading occurs at late ages, as the microstructure does not evolve much once loaded. However, at early ages, once creep starts, the strain evolution is different: The compliance functions do not even share the same tangent. This a priori nonintuitive result [for several examples of composites exhibiting only solidification, both compliance functions are found to have the same initial tangent

(Sanahuja 2014)] seems to be the consequence of the anhydrous dissolution process. Li et al. (2015b) noticed the same effect on full-field simulations and called it apparent viscoelastic relaxation.

A simple one-dimensional (1D) model, inspired by the solidification theory, can help to get an idea of the influence of dissolution. A parallel arrangement of elastic (Young's modulus E_s) dissolving layers is considered. The solid volume fraction is thus a decreasing function of time t , denoted $f_s(t)$. The applied uniaxial stress is a step, as $\Sigma(t) = \Sigma_0 H(t - t')$, the loading time t' being a parameter. The stress in the remaining solid phase is thus $\sigma(t) = \Sigma(t)/f_s(t)$. The strain in the solid phase is also the macroscopic strain, due to the parallel arrangement: $E(t) = \varepsilon(t) = \Sigma_0 H(t - t') / [E_s f_s(t)]$. As $f_s(t)$ decreases, the macroscopic strain $E(t)$ increases for $t > t'$, while the macroscopic strain for a frozen microstructure stays at $E^{\text{frozen}}(t) = \Sigma_0 H(t - t') / [E_s f_s(t')]$ [Fig. 8(b)]. Note that the strain rates at loading ($t'/\tau = 1$) are clearly different.

The approach proposed to homogenize evolving microstructures is illustrated on a representation of cement paste, which is too simplified to allow a quantitative comparison of aging creep functions to experimental results. Still, for future reference, bibliographic sources providing creep behavior of cement pastes aforementioned in the subsection regarding hydrates behavior, are recalled here. Le Roy (1995) measured basic creep of cement pastes at 28 days and of concretes at various loading ages. Use of the latter data for validation would require an additional upscaling step, from cement paste to concrete. As morphology does not evolve at the concrete scale, this upscaling is straightforward following Sanahuja (2013), once a concrete morphological model (which may include interfacial transition zones) has been defined. Briffaut et al. (2012) also provide creep results at concrete scale. Tamtsia et al. (2004) provide basic creep curves of cement pastes loaded at 18, 24, and 30 h. Irfan-ul-Hassan et al. (2016) propose an extensive characterization of the first minutes of creep functions of cement pastes through repeated short tests on the same sample.

Qualitatively, the creep functions estimated considering microstructure evolution [plain lines in Fig. 8(a)] are closer to the experimental results of Tamtsia et al. (2004) (Fig. 6 on the referenced paper) than those estimated considering frozen microstructure [dashed lines in Fig. 8(a)]. Indeed, the experimental creep strain rate is high at the onset, then decreases as a function of time (creep functions show a significant downward concavity).

Conclusion and Prospects

An approach to upscale the mechanical behavior of composite materials undergoing geometrical evolutions of their microstructure

is proposed, with preliminary applications to cement pastes. Mean field homogenization is considered. Both elastic and nonaging viscoelastic behaviors are considered for the phases. While the evolving nature of microstructure does not prevent the use of mean-field homogenization in the case of elastic phases, special care has to be taken for viscoelastic phases. Indeed, time appears both in the elementary behaviors and in the evolution of microstructure. Even if the phases are nonaging, the effective behavior is aging viscoelastic.

A common approach, considering microstructure as frozen once the macroscopic loading step has been applied, allows for approximating the effective aging behavior using readily available tools (namely the correspondence principle with the Laplace-Carson transform), when phases are nonaging. The originality of the paper resides in the approach proposed to overcome this assumption. Extending Bažant's solidification theory, an equivalent composite is built, whose microstructure is constant but made up of aging linear viscoelastic fictitious phases. Taking advantage of recent advances in aging linear viscoelastic homogenization, the effective behavior of this equivalent composite can then be estimated. Note that this approach is not restricted to nonaging phases in the evolving microstructure: aging phases are as straightforward to consider. The frozen microstructure assumption is, as expected, found to be valid only for late-age loadings, once the microstructure evolution becomes negligible. When loaded at early age, compliance functions from both techniques (with and without this frozen assumption) only share the initial elastic strain. Even the initial strain rate is different. This is attributed to the dissolution process. Qualitatively, compliance functions from evolving microstructure are closer to the experimental ones reported in Tamtsia et al. (2004).

The proposed application to cement paste is deliberately crude to focus on the description of the homogenization approach rather than on unnecessary technical details. However, before further comparisons to experimental data, the model should be improved in several aspects:

- Hydration kinetics: More realistic hydration kinetics should be used, either coming from experimental measurements or from hydration models. Moreover, the various anhydrous and hydrated phases could be detailed;
- Morphological model: Morphologies that have been successfully used to estimate other mechanical properties (stiffness, strength, nonaging creep) can be adapted in the aging viscoelastic context proposed here. Some of these models include features (multiscale representation, aspherical shapes) that have proven to reduce shortcomings on prediction of the setting hydration degree;
- Elementary viscoelastic behavior of C-S-H: More realistic behaviors should be used, for example, obtained from the scale where sliding interfaces can be explicitly described;
- Stress state of anhydrous and hydrates: A study of the influence of the stress state over dissolution and precipitation processes should be performed, and also the zero-stress assumption for hydrates precipitating in confined spaces should be overcome; and
- Aging mechanisms: As concrete experimentally shows aging creep even for loadings at long term [typically several years, see e.g., data reported by Bažant (1975, 1988)], mechanisms other than hydration should be taken into account.

among these prospects, modifications of hydration kinetics or viscoelastic behavior of hydrates can be straightforwardly taken into account by the proposed approach. Indeed, it is modular enough to use as inputs any kinetics curve and any linear viscoelastic behavior, defined by compliance or relaxation functions, for elementary phases. Improving the morphological model requires the extension

of Sanahuja (2013) to a spheroidal inhomogeneity [see Lavergne et al. (2016) in the case of a constant Poisson ratio for the matrix] and to a multilayered composite sphere.

As shown in Honorio et al. (2016), further improvements of the approach proposed here and applications to concrete are already promising.

References

- Abate, J., and Whitt, W. (2006). "A unified framework for numerically inverting Laplace transforms." *INFORMS J. Comput.*, 18(4), 408–421.
- Avramov, I. (2007). "The role of stress development and relaxation on crystal growth in glass." *J. Non-Crystalline Solids*, 353(30–31), 2889–2892.
- Azenha, M., Magalhães, F., Faria, R., and Cunha, A. (2010). "Measurement of concrete E-modulus evolution since casting: A novel method based on ambient vibration." *Cem. Concr. Res.*, 40(7), 1096–1105.
- Bažant, Z. (1972). "Numerical determination of long-range stress history from strain history in concrete." *Mater. Struct.*, 5(3), 135–141.
- Bažant, Z. (1975). "Theory of creep and shrinkage in concrete structures: A precis of recent developments." *Mech Today*, 2, 1–93.
- Bažant, Z. (1977). "Viscoelasticity of solidifying porous material—Concrete." *J. Eng. Mech. Div.*, 103(6), 1049–1067.
- Bažant, Z. (1979). "Thermodynamics of solidifying or melting viscoelastic material." *J. Eng. Mech. Div.*, 105(6), 933–952.
- Bažant, Z. (1988). "Material models for structural creep analysis." *Mathematical modeling of creep and shrinkage of concrete*, Wiley, Chichester, U.K., 99–215.
- Bažant, Z. (2001). "Prediction of concrete creep and shrinkage: Past, present and future." *Nucl. Eng. Des.*, 203(1), 27–38.
- Bažant, Z., and Prasanna, S. (1989). "Solidification theory of concrete creep. I: Formulation." *J. Eng. Mech.*, 10.1061/(ASCE)0733-9399(1989)115:8(1691), 1691–1703.
- Bernard, O., Ulm, F.-J., and Lemarchand, E. (2003). "A multiscale micromechanics-hydration model for the early-age elastic properties of cement-based materials." *Cem. Concr. Res.*, 33(9), 1293–1309.
- Boumiz, A., Vernet, C., and Cohen Tenoudji, F. (1996). "Mechanical properties of cement pastes and mortars at early ages: Evolution with time and degree of hydration." *Adv. Cem. Based. Mater.*, 3(3–4), 94–106.
- Briffaut, M., Benboudjema, F., Torrenti, J.-M., and Nahas, G. (2012). "Concrete early age basic creep: Experiments and test of rheological modelling approaches." *Constr. Build. Mater.*, 36, 373–380.
- Budiansky, B. (1965). "On the elastic moduli of some heterogeneous materials." *J. Mech. Phys. Solids*, 13(4), 223–227.
- Byfors, J. (1980). "Plain concrete at early ages." *Technical Rep.*, Swedish Cement and Concrete Research Institute, Stockholm, Sweden.
- Carol, I., and Bažant, Z. (1993). "Viscoelasticity with aging caused by solidification of nonaging constituent." *J. Eng. Mech.*, 10.1061/(ASCE)0733-9399(1993)119:11(2252), 2252–2269.
- Constantinides, G., and Ulm, F.-J. (2004). "The effect of two types of C-S-H on the elasticity of cement-based materials: Results from nano-indentation and micromechanical modelling." *Cem. Concr. Res.*, 34(1), 67–80.
- Correns, C. (1949). "Growth and dissolution of crystals under linear pressure Spec." *Discuss. Faraday Soc.*, 5, 267–271.
- Diamond, S. (2004). "The microstructure of cement paste and concrete—A visual primer." *Cem. Concr. Compos.*, 26(8), 919–933.
- Dormieux, L., Kondo, D., and Ulm, F.-J. (2006). *Microporomechanics*, Wiley, Chichester, U.K.
- Eshelby, J. D. (1957). "The determination of the elastic field of an ellipsoidal inclusion, and related problems." *Proc. R. Soc. London, Ser. A, Math. Phys. Sci.*, 241(1226), 376–396.
- Gaver, D. P. (1966). "Observing stochastic processes and approximate transform inversion." *Oper. Res.*, 14(3), 444–459.
- Gu, S., Bary, B., He, Q.-C., and Thai, M.-Q. (2012). "Multiscale poro-creep model for cement-based materials." *Int. J. Numer. Anal. Methods Geomech.*, 36(18), 1932–1953.

- Hill, R. (1965). "A self-consistent mechanics of composite materials." *J. Mech. Phys. Solids*, 13(4), 213–222.
- Honorio, T., Bary, B., and Benboudjema, F. (2016). "Multiscale estimation of ageing viscoelastic properties of cement-based materials: A combined analytical and numerical approach to estimate the behaviour at early age." *Cem. Concr. Res.*, 85, 137–155.
- Irfan-ul-Hassan, M., Pichler, B., Reihnsner, R., and Hellmich, C. (2016). "Elastic and creep properties of young cement paste, as determined from hourly repeated minute-long quasi-static tests." *Cem. Concr. Res.*, 82, 36–49.
- Juenger, M., Lamour, V., Monteiro, P., Gartner, E., and Denbeaux, G. (2003). "Direct observation of cement hydration by soft X-ray transmission microscopy." *J. Mater. Sci. Lett.*, 22(19), 1335–1337.
- Lavergne, F., Sab, K., Sanahuja, J., Bornert, M., and Toulemonde, C. (2016). "Homogenization schemes for aging linear viscoelastic matrix-inclusion composite materials with elongated inclusions." *Int. J. Solids Struct.*, 80, 545–560.
- Le, Q., Meftah, F., He, Q.-C., and Le Pape, Y. (2007). "Creep and relaxation functions of a heterogeneous viscoelastic porous medium using the mori-tanaka homogenization scheme and a discrete microscopic retardation spectrum." *Mech. Time-Depend Mater.*, 11(3), 309–331.
- Le Roy, R. (1995). "Déformations instantanées et différées des bétons à hautes performances." Ph.D. thesis, Ecole Nationale des Ponts et Chaussées (ENPC), Champs-sur-Marne, France.
- Li, X., Grasley, Z., Garboczi, E., and Bullard, J. (2015a). "Computing the time evolution of the apparent viscoelastic/viscoplastic poisson's ratio of hydrating cement paste." *Cem. Concr. Compos.*, 56, 121–133.
- Li, X., Grasley, Z., Garboczi, E., and Bullard, J. (2015b). "Modeling the apparent and intrinsic viscoelastic relaxation of hydrating cement paste." *Cem. Concr. Compos.*, 55, 322–330.
- Lothenbach, B., Scrivener, K., and Hooton, R. (2011). "Supplementary cementitious materials." *Cem. Concr. Res.*, 41(12), 1244–1256.
- Lothenbach, B., and Winnefeld, F. (2006). "Thermodynamic modelling of the hydration of portland cement." *Cem. Concr. Res.*, 36(2), 209–226.
- Maia, L., Azenha, M., Faria, R., and Figueiras, J. (2012a). "Identification of the percolation threshold in cementitious pastes by monitoring the E-modulus evolution." *Cem. Concr. Compos.*, 34(6), 739–745.
- Maia, L., Azenha, M., Geiker, M., and Figueiras, J. (2012b). "E-modulus evolution and its relation to solids formation of pastes from commercial cements." *Cem. Concr. Res.*, 42(7), 928–936.
- Mandel, J. (1966). *Cours de mécanique des milieux continus*, Gauthier-Villars, Sceaux, Paris.
- Masson, R., Brenner, R., and Castelnaud, O. (2012). "Incremental homogenization approach for ageing viscoelastic polycrystals." *Comptes Rendus Mécanique*, 340(4–5), 378–386.
- Pichler, B., et al. (2013). "Effect of gel-space ratio and microstructure on strength of hydrating cementitious materials: An engineering micromechanics approach." *Cem. Concr. Res.*, 45, 55–68.
- Pichler, B., and Hellmich, C. (2011). "Upscaling quasi-brittle strength of cement paste and mortar: A multi-scale engineering mechanics model." *Cem. Concr. Res.*, 41(5), 467–476.
- Pichler, B., Hellmich, C., and Eberhardsteiner, J. (2009). "Spherical and acicular representation of hydrates in a micromechanical model for cement paste: Prediction of early-age elasticity and strength." *Acta Mech.*, 203(3–4), 137–162.
- Powers, T. C., and Brownyard, T. L. (1946). "Studies of the physical properties of hardened portland cement paste (nine parts)." *J. Am. Concr. Inst.*, 43(9), 101–132.
- Ricaud, J.-M., and Masson, R. (2009). "Effective properties of linear viscoelastic heterogeneous media: Internal variables formulation and extension to ageing behaviours." *Int. J. Solids Struct.*, 46(7), 1599–1606.
- Richardson, I. G. (2000). "The nature of the hydration products in hardened cement pastes." *Cem. Concr. Compos.*, 22(2), 97–113.
- Rossi, P., Tailhan, J.-L., Le Maou, F., Gaillet, L., and Martin, E. (2012). "Basic creep behavior of concretes investigation of the physical mechanisms by using acoustic emission." *Cem. Concr. Res.*, 42(1), 61–73.
- Sanahuja, J. (2013). "Effective behaviour of ageing linear viscoelastic composites: Homogenization approach." *Int. J. Solids Struct.*, 50(19), 2846–2856.
- Sanahuja, J. (2014). "Homogenization of solidifying random porous media: Application to ageing creep of cementitious materials." *RILEM Int. Symp. on Concrete Modelling*, Tsinghua Univ., Beijing.
- Sanahuja, J., and Di Ciccio, M. (2015). "From micromechanisms to mechanical behaviour: An application to ageing creep of a cement paste." *Mechanics and physics of creep, shrinkage, and durability of concrete and concrete structures*, ASCE, Reston, VA.
- Sanahuja, J., and Dormieux, L. (2010). "Creep of a C-S-H gel: Micromechanical approach." *Int. J. Multiscale Comput. Eng.*, 8(4), 357–368.
- Sanahuja, J., Dormieux, L., and Chanvillard, G. (2007). "Modelling elasticity of a hydrating cement paste." *Cem. Concr. Res.*, 37(10), 1427–1439.
- Sanahuja, J., Dormieux, L., and Chanvillard, G. (2008). "A reply to the discussion 'Does C-S-H particle shape matter?'" F.-J. Ulm and H. M. Jennings of the paper "Modelling elasticity of a hydrating cement paste." *Cem. Concr. Res.*, 38(8–9), 1130–1134.
- Sanahuja, J., Dormieux, L., Le Pape, Y., and Toulemonde, C. (2009). "Modélisation micro-macro du fluage propre du béton." 19^e congrès français de mécanique, AFM, Maison de la Mécanique, Courbevoie, France.
- Scheiner, S., and Hellmich, C. (2009). "Continuum microviscoelasticity model for aging basic creep of early-age concrete." *J. Eng. Mech.*, 10.1061/(ASCE)0733-9399(2009)135:4(307), 307–323.
- Scherer, G. (1999). "Crystallization in pores." *Cem. Concr. Res.*, 29(8), 1347–1358.
- Scherer, G. (2004). "Stress from crystallization of salt." *Cem. Concr. Res.*, 34(9), 1613–1624.
- Shahidi, M., Pichler, B., and Hellmich, C. (2014). "Viscous interfaces as source for material creep: A continuum micromechanics approach." *Eur. J. Mech. A/Solids*, 45, 41–58.
- Shahidi, M., Pichler, B., and Hellmich, C. (2016). "Interfacial micromechanics assessment of classical rheological models. I: Single interface size and viscosity." *J. Eng. Mech.*, 10.1061/(ASCE)EM.1943-7889.0001012, 04015092.
- Smilauer, V., and Bažant, Z. (2010). "Identification of viscoelastic C-S-H behavior in mature cement paste by FFT-based homogenization method." *Cem. Concr. Res.*, 40(2), 197–207.
- Stefan, L., Benboudjema, F., Torrenti, J.-M., and Bissonnette, B. (2010). "Prediction of elastic properties of cement pastes at early ages." *Comput. Mater. Sci.*, 47(3), 775–784.
- Stehfest, H. (1970). "Algorithm 368: Numerical inversion of Laplace transforms." *Commun. Assoc. Comput. Mach.*, 13(1), 47–49.
- Stora, E., He, Q., and Bary, B. (2006). "Influence of inclusion shapes on the effective linear elastic properties of hardened cement pastes." *Cem. Concr. Res.*, 36(7), 1330–1344.
- Sun, Z., Ye, G., and Shah, S. P. (2005). "Microstructure and early-age properties of portland cement paste—Effects of connectivity of solid phases." *ACI Mater. J.*, 102(2), 122–129.
- Tamtsia, B. T., and Beaudoin, J. J. (2000). "Basic creep of hardened cement paste, a re-examination of the role of water." *Cem. Concr. Res.*, 30(9), 1465–1475.
- Tamtsia, B. T., Beaudoin, J. J., and Marchand, J. (2004). "The early age short-term creep of hardening cement paste: Load-induced hydration effects." *Cem. Concr. Compos.*, 26(5), 481–489.
- Taplin, J. (1959). "A method for following the hydration reaction in portland cement paste." *Aust. J. Appl. Sci.*, 10(3), 329–345.
- Termkhajornkit, P., Vu, Q., Barbarulo, R., Daronnat, S., and Chanvillard, G. (2014). "Dependence of compressive strength on phase assemblage in cement pastes: Beyond gel-space ratio—Experimental evidence and micromechanical modeling." *Cem. Concr. Res.*, 56, 1–11.
- Torrenti, J.-M., and Benboudjema, F. (2005). "Mechanical threshold of cementitious materials at early age." *Mater. Struct.*, 38(3), 299–304.
- Velez, K., Maximilien, S., Damidot, D., Fantozzi, G., and Sorrentino, F. (2001). "Determination by nanoindentation of elastic modulus and hardness of pure constituents of portland cement clinker." *Cem. Concr. Res.*, 31(4), 555–561.
- Velez, K., and Sorrentino, F. (2001). "Characterization of cementitious materials by nanoindentation." *Kurdowski Symp. on Science of Cement and Concrete*, Akapit-Wydaw, Naukowe, 67–77.

- Volterra, V. (1887). "Sopra le funzioni che dipendono da altre funzioni." *Rendiconti della Reale Accademia dei Lincei*, 4(3), 97–105.
- Volterra, V. (1959). *Theory of functionals and of integral and integro-differential equations (1925 Madrid lectures)*, Dover, New York.
- Wittmann, F. H. (1982). "Creep and shrinkage mechanisms." *Creep and shrinkage in concrete structures*, Z. P. Bažant and F. H. Wittmann, eds., Wiley, New York, 129–161.
- Zaoui, A. (2002). "Continuum micromechanics: Survey." *J. Eng. Mech.*, 10.1061/(ASCE)0733-9399(2002)128:8(808), 808–816.